Bull Volcanol (2012) 74:579–587
DOI 10.1007/s00445-011-0548-y

RESEARCH ARTICLE

Rapid, low-cost photogrammetry to monitor volcanic eruptions: an example from Mount St. Helens, Washington, USA

Angela K. Diefenbach · Juliet G. Crider · Steve P. Schilling · Daniel Dzurisin

Received: 19 April 2011 / Accepted: 27 August 2011 / Published online: 21 October 2011

Abstract We describe a low-cost application of digital photogrammetry using commercially available photogrammetric software and oblique photographs taken with an off-the-shelf digital camera to create sequential digital elevation models (DEMs) of a lava dome that grew during the 2004–2008 eruption of Mount St. Helens (MSH) volcano. Renewed activity at MSH provided an opportunity to devise and test this method, because it could be validated against other observations of this well-monitored volcano. The datasets consist of oblique aerial photographs (snapshots) taken from a helicopter using a digital single-lens reflex camera. Twelve sets of overlapping digital images of the dome taken during 2004–2007 were used to produce DEMs and to calculate lava dome volumes and extrusion rates. Analyses of the digital images were carried out using photogrammetric software to produce three-dimensional coordinates of points identified in multiple photos. The evolving morphology of the dome was modeled by comparing successive DEMs. Results were validated by comparison to volume measurements derived from traditional vertical photogrammetric surveys by the US Geological Survey Cascades Volcano Observatory. Our technique was significantly less expensive and required less time than traditional vertical photogrammetric techniques; yet, it consistently yielded volume estimates within 5% of the traditional method. This technique provides an inexpensive, rapid assessment tool for tracking lava dome growth or other topographic changes at restless volcanoes.

Keywords Oblique photogrammetry · Dome growth · Eruption monitoring · Volume calculations · Mount St. Helens

Editorial responsibility: R. Cioni

Electronic supplementary material The online version of this article (doi:10.1007/s00445-011-0548-y) contains supplementary material, which is available to authorized users.

A. K. Diefenbach · J. G. Crider
Department of Geology, Western Washington University, Bellingham, WA, USA

A. K. Diefenbach (✉) · S. P. Schilling · D. Dzurisin
Cascades Volcano Observatory, U.S. Geological Survey, 1300 SE Cardinal Court, Vancouver, WA 98683, USA
e-mail: adiefenbach@usgs.gov

J. G. Crider
Department of Earth and Space Sciences, University of Washington, Seattle, WA, USA

Introduction

Measurements of lava volume and extrusion rate during a volcanic eruption can be used to constrain models of eruption dynamics that are based on other monitoring techniques such as volcanic gas emission, geochemistry, seismicity, and geodesy (Stevens 2002; Wadge 2003; Iverson et al. 2006; Iverson 2008). The volume of lava and the rate at which it is extruded, in the form of flows or domes, are indicators of the amount of magma stored in a volcanic system, the plumbing system, and potential eruption duration (e.g., Zlotnicki et al. 1990; Harris et al. 2000, 2003; Kaneko et al. 2002; Stevens 2002; Wadge et al. 2006). In addition, monitoring the volumetric change and extrusion rate of an actively growing dome provides critical information for the effective assessment of volcanic hazards (e.g., Calder et al. 2002).

Photogrammetry is one technique used to measure lava volume that provides quantitative, three-dimensional spatial

information from remote imagery. Rather than single-point measurements of surface deformation from instruments such as Global Positioning System receivers, electronic distance meters, tiltmeters, and strainmeters, photogrammetry offers the advantages of broad spatial coverage and remote data acquisition. Photogrammetry also offers relatively low cost and ease of image processing when compared to other synoptic measurement techniques (e.g., interferometric synthetic aperture radar and airborne laser swath mapping or LiDAR). Moreover, data acquisition is flexible over a wide range of time scales. However, photogrammetry generally produces a lower resolution of ground movements than ground-based surveying techniques.

Digital elevation models (DEMs) made from vertical air photos taken from low-flying aircraft are the most common products derived by photogrammetric techniques applied within volcanology (e.g., Moore and Albee 1981; Mills 1992; Achilli et al. 1998; Baldi et al. 2000, 2002; Schilling et al. 2004, 2008; Thompson and Schilling 2007). Comparison of DEMs constructed from photos taken on successive dates can be used to study and monitor crustal deformation and extrusion of lava. Deformation patterns, displacement vectors, volumes and extrusion rates derived from DEMs, provide quantitative information on the geomorphic evolution of a volcano (e.g., Jordan and Kieffer 1981; Achilli et al. 1998; Baldi et al. 2000; Kerle 2002; Pyle and Elliott 2006; Cecchi et al. 2003; Schilling et al. 2008).

In the last few decades, advances in computer systems and software have moved photogrammetry from analogue to digital format. In volcano monitoring, where time is critical, digital photogrammetry permits near-real-time, precise measurements of both broad-scale and local surface change (e.g., Honda and Nagai 2002; Bluth and Rose 2004). Digital techniques also facilitate interpretation of oblique airborne and ground-based (terrestrial) photographs. For example, Baldi et al. (2000) and Julio-Miranda and Delgado-Granados (2003) used digital photogrammetry to successfully monitor landslides and glaciers on volcanoes for hazard mitigation purposes. Surveys by James and colleagues (2006, 2007) employed terrestrial photogrammetry to measure and monitor active lava flows and spatially reference thermal imagery. At Soufrière Hills Volcano, Herd et al. (2005) used terrestrial photogrammetry to build DEMs to measure collapse-scar volumes and Ryan et al. (2010) used single images to derive volumes and extrusion rates during phase 3 of the eruption. Oblique images have been used to track three-dimensional vector displacements at volcanoes (Major et al. 2009) as well as to determine rapid changes in volcano topography from image sequence matching (Cecchi et al. 2003).

Here, we describe a low-cost method of photogrammetry, applied to Mount St. Helens (MSH) volcano. Recent eruptive activity at MSH provides an opportunity to devise and test methods for volcano monitoring by making observations at an accessible, well-instrumented volcano. We employ an off-the-shelf digital camera, commercially available software and a laptop computer to rapidly produce three-dimensional models of the extruded lava at MSH, for several dates spanning more than 2 years. The sequence of models is used to estimate dome volumes and time-averaged extrusion rates and are validated by comparison to the same parameters determined by traditional vertical photogrammetry.

The 2004–2008 eruption OF MSH

In October 2004, MSH began erupting again after nearly 18 years of eruptive quiescence. Dome growth at MSH during the 2004–2008 eruption was characterized by the extrusion and collapse of solid dacite spines (Scott et al. 2008). The eruption produced a series of seven spines that extruded from a vent directly south of the previously extruded dome (1980–1986) and through a crater glacier (Schilling et al. 2008; Scott et al. 2008; Vallance et al. 2008). The dome grew continuously from October 2004 to the end of the eruption in January 2008, through a combination of exogenous and endogenous growth (Major et al. 2009). Following Vallance et al. (2008), spines 1 and 2 (minor in size) extruded in October 2004, followed by spines 3 and 4 that extruded southward, until collision with the crater wall caused the spines to break apart (between late October 2004 and April 2005), and get shoved eastward by spine 5, which continued to issue from the vent (Scott et al. 2008; Vallance et al. 2008; Fig. 1a–c). Between April and August 2005 spine 5 grew and fell apart (Fig. 1c). Spine 6 followed in October 2005, but was rapidly overtaken by spine 7; a combination of several spines that transitioned to endogenous growth and formed a broad, composite mass (Vallance et al. 2008; Fig. 1d). Spine 7 grew continuously until January 2008 (Major et al. 2009).

The 2004–2008 eruption of MSH was well-monitored by a suite of techniques, both traditional and novel. Photogrammetry proved vital in characterizing the evolution of dome growth through time. Time-lapse cameras were installed in several locations on the crater rim to document the nature and pace of the eruption (Major et al. 2008, 2009; Poland et al. 2008). In addition, traditional aerial photogrammetry was used to estimate dome volume and extrusion rates throughout the eruption. In total, 27 DEMs were derived from vertical aerial photographs taken at intervals of approximately 3 weeks between 2004 and 2007 (Schilling et al. 2008). This work provides an important baseline for comparison to our study.

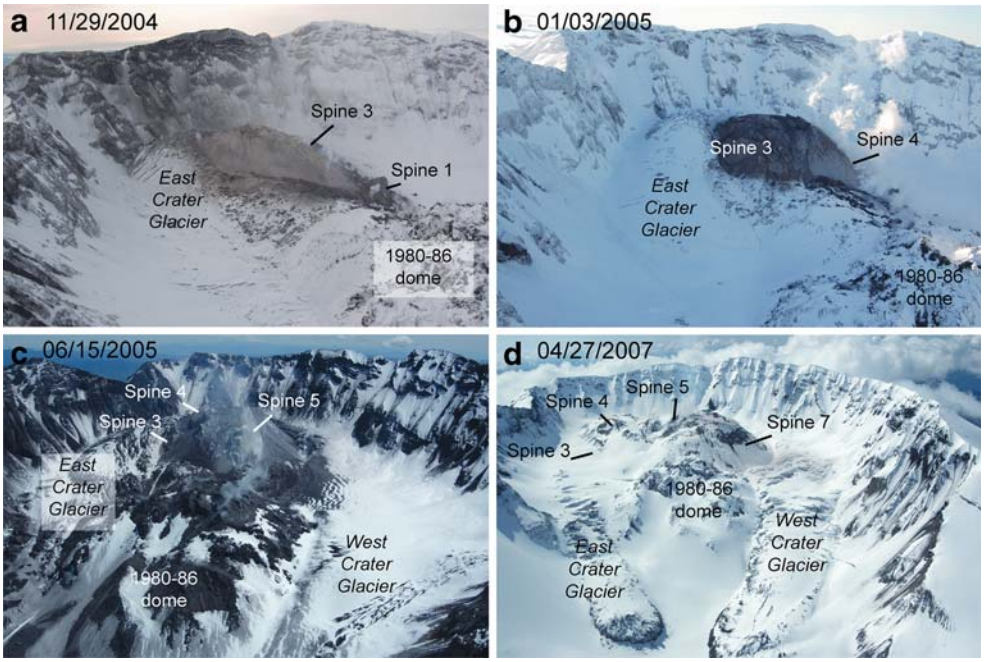

Fig. 1 Series of oblique photographs taken from a helicopter depicting dome growth in the form of a series of lava spines in the crater of Mount St. Helens. **a** View to the west–southwest of spine 3. **b** *Spine 4* overtopping the remnants of *spine 3* and pushing against the south crater wall. This view is to the west-southwest. **c** Mid-stage of growth of *spine 5* with remnants of spine 3 and 4 to the east of active lava extrusion. This view is to the south. **d** Final set of oblique photographs in April 2007 (view to the south); the broad composite mass of *spine 7* dominates the crater area south of 1980–1986 dome

Oblique photogrammetry

Data acquisition

Image datasets were collected on 12 dates (Table 1) between November 2004 and April 2007. Helicopter flights for oblique photogrammetry were scheduled on the same day or within a few days of vertical aerial photography flights, to enable direct comparison of the two approaches to measuring dome growth (see Discussion). Images were acquired with a digital SLR camera (Nikon D70,[1] 6.1 megapixel sensor) with a 17- to 55-mm lens set to the widest focal length and focused at infinity to provide a wide-angle field of view and to maintain consistency while acquiring images. Helicopter flights followed a rectangular path over the volcano as viewed from above, increasing in altitude for each repeat circuit. This technique provided several sets of photographs, each with a different viewing angle and single-image field of view. Images were acquired with an average 60% overlap to facilitate identification of common features between photographs. Camera calibration was performed using a built-in extension of the photogrammetric software and a suite of photographs taken at different angles of a gridded calibration target.

Photogrammetric analysis

We used PhotoModeler Pro® (EOS Systems Inc.) software for our analyses. For each date on which images were acquired, four to seven images were selected based on percentage of overlap, optimum angle of convergence (45°), area of the dome visible within each photo, and inclusion of ground control points (GCPs) (Fig. 2a). A minimum of four GCPs were identified in each model to obtain external geometry (spatial location and orientation) of the camera at the time that each image was acquired. Due to hazardous conditions at the volcano, suitable control points were extracted from a high-resolution (area of each cell is 4 m^2, herein referred to as 2 m cell size) DEM of well-defined natural features that were clearly identifiable in adjacent photographs. Relative orientation of each model was established by identifying at least six homologous tie points used to calculate the projective centers of the images. The identification of GCPs and tie points orient each model from an arbitrary spatial coordinate system to an accurately referenced three-dimensional reference frame. Each photogrammetric model was constructed from a cloud of three-dimensional points (referred to as reference points). These points were manually identified between pairs or series of photographs and were typically recognizable point features such as intersections of cracks, edges of large talus blocks, and striae. As the density of reference points on the dome increased, so did the accuracy of representation of the dome's surface.

Volume and extrusion calculations

Our principal goals were to quantify the volume of erupted material for each date of oblique photography and produce a time series of average extrusion rate between successive volume estimates. Photogrammetric models were exported

[1] Use of trade names in this manuscript is for identification purposes only and does not constitute endorsement by the US Geological Survey.

Table 1 Calculated dome volume and lava flux rate of the MSH eruption from November 2004 through April 2007

Date of oblique photography	Dome volume (10^6 m^3)	Extrusion rate (m^3/s)
11/20/2004	15±0.1	4.3±0.0
11/29/2004	22±0.2	(9.2±0.3)
		5.2±0.1[a]
01/03/2005	26±0.4	1.3±0.1
02/01/2005	35±0.2	3.6±0.2
02/22/2005	38±0.4	1.7±0.2
03/11/2005	41±0.7	2.0±0.6
04/10/2005	47±0.8	2.3±0.4
05/12/2005	56±0.3	3.3±0.3
06/15/2005	60±0.4	1.4±0.2
10/12/2005	68±0.3	0.8±0.1
05/30/2006	85±0.8	0.9±0.0
04/20/2007	94±0.9	0.3±0.0

Associated error estimates are rounded to one significant figure

[a]Extrusion rate recalculated without using data from 11/20/2004. This value used when graphing extrusion rate vs. time. Volume estimates for 11/20/2004 were determined to be too low (see text), which adds uncertainty to the time-averaged extrusion rate on 11/29/2004.

as ASCII text files (*x*, *y*, *z* of each point) for import into geographic information system (GIS). Using GIS, we generated a triangulated irregular network (TIN) for each model by means of a Delaunay triangulation, where reference points are vertices for triangular facets. The TINs were interpolated to raster DEMs with a 2 m cell size, a resolution equivalent to the 1986 and 2004–2007 DEMs produced by the USGS (Fig. 2b).

A 1986 DEM of the pre-eruption surface served as a basal surface for volume calculations because this vintage of DEM was made before the growth of a glacier (1996–present; Schilling et al. 2004) that masks the crater floor

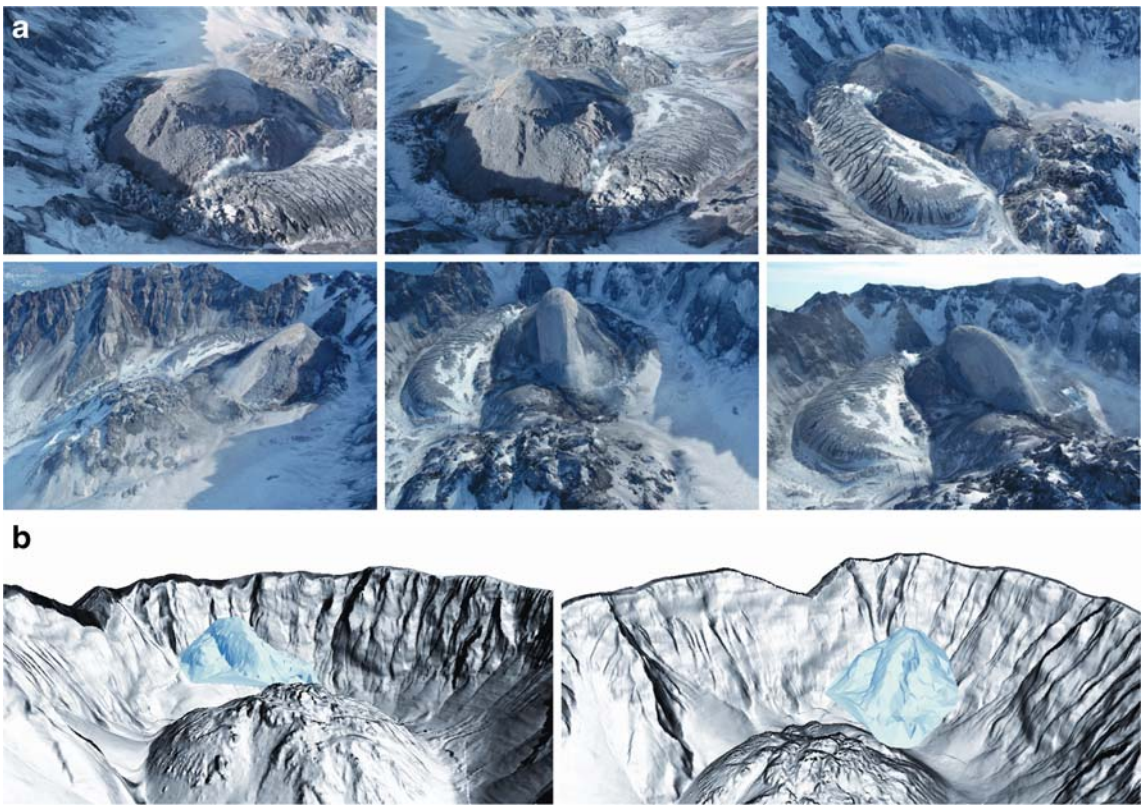

Fig. 2 **a** Series of oblique photographs taken 22 February 2005 used for photogrammetric analyses. **b** Photogrammetric results in the form of shaded relief depictions of DEMs for 22 February 2005 (*blue scale*). 1986 DEM (*gray scale*) is used for local reference of crater wall and 1980–1986 dome

topography. Volume estimates were calculated by subtracting the 1986 DEM from each 2004–2007 oblique photogrammetric DEM. The elevation difference between corresponding cells of the DEMs was calculated, and this difference was multiplied by the area of each cell (4 m^2). The sum of these calculations for all cells yielded an estimate of the total volume of extruded lava. Time-averaged extrusion rates were calculated by dividing the net volume change by the elapsed time between successive sets of photographs.

Volume estimates were complicated by the presence of Crater Glacier through which the 2004–2008 lava dome emerged. The distribution of extruded rock masked by the glacier presents perhaps the largest source of potential error when calculating extruded rock volumes. For consistency, volumes reported here were calculated by projecting the perimeter of the visible extruded lava vertically downward to the 1986 basal surface.

Error estimation

Photogrammetric precision achieved in each model is examined via the root mean square (RMS) residual. RMS residuals represent the difference between an operator-selected reference point and the expected coordinates calculated by the software. The location calculated by the software is defined by the projection and control points. If the ground control used to orient the model has error, this error gets carried on to the residuals of reference points that make up the model. Estimated uncertainty in locating GCPs in photographs and using aerotriangulation is 0.17 m RMS residual (Schilling et al. 2008). RMS residuals reported by the photogrammetry software were converted from pixels to meters by estimating the ground sample distance (GSD) for each model. Accurate estimates of GSD are difficult to achieve from oblique photographs, because there may be a large difference in scale between foreground and background. As a result, pixels in different parts of an image can represent much different areas (i.e., length × width) on the ground. To produce a first-order estimate of the average GSD for a given DEM, we averaged GSDs for individual pixels from a sample of locations in the area of interest for each model. The RMS value in pixels was multiplied by the average GSD to estimate an RMS residual in meters. The average estimated RMS residual for the DEMs created for this study is 1.3 m. This estimate is based on the output provided by the photogrammetric software and does not include the additional RMS error associated with the GCPs extracted from the 2 m DEM.

We propagated the RMS residuals and uncertainty in the GSD estimates throughout our calculations to estimate the formal uncertainty (precision) of our dome volume and extrusion rate measurements (Table 1). On average, we estimate the uncertainty in dome volume to be 4.3×10^5 m^3 (less than 1% of the average dome volume). Differencing values increases the relative uncertainty. We estimate the average uncertainty in volume change between successive DEMs to be 5.7×10^5 m^3 (about 6% of the average volume change). Schilling and colleagues (2008) estimated the formal uncertainty of volume change estimates in their vertical photogrammetric method to be 4%.

The error associated with the extrusion rate values derived from the estimated volumes for each DEM were calculated using standard error propagation methods (e.g., Stoer and Bulirsch 2002). The time uncertainty is the sum of the durations of photo acquisition for the two dates included in each calculation. The average extrusion rate uncertainty is 0.19 m^3/s; approximately7% of the average extrusion rate (Table 1).

Additional detail related to the methodology is given in Appendix 1 and by Diefenbach (2007).

Results

Twelve DEMs of the growing lava dome inside the crater of MSH were constructed from oblique photographs taken between November 20, 2004 and April 20, 2007 (Fig. 3a–l). During this time, dome growth was continuous. The models were also used to track the morphological evolution of the dome. Dome growth can be categorized in two distinct phases; the first dominated by rapid exogenous growth and eastward migration of the extruded spines, and a second governed by slower, increasingly endogenous growth and westward migration of the spines.

By the time the first set of oblique photographs was acquired, dome growth had already produced two small spines (1 and 2), and a third was being extruded. The first date of oblique photography, November 20, 2004, yielded a dome volume estimate of 15×10^6 m^3 (Figs. 3a and 4). Persistent steaming at the vent obstructed views of nearly the entire west and north side of the dome, and no images were captured from the southern end of the dome. The volume estimate for this date is likely an underestimate because of this limited coverage. Nine days later on November 29, oblique photographs included the entire dome and our volume estimate is 22×10^6 m^3 (Figs. 3b and 4). The previous volume underestimate leads to a likely overestimate of extrusion rate over this time interval (9.0 m^3/s; Table 1). April 10, 2005 images capture the final breakup of spine 4 (Fig. 3g). By May 12, 2005, the extrusion rate was 3.3 m^3/s and the estimated dome volume was 56×10^6 m^3 (Figs. 3h and 4). Dome height had reached an apex of 371 m above the 1986 crater floor with growth of spine 5 (Fig. 3h).

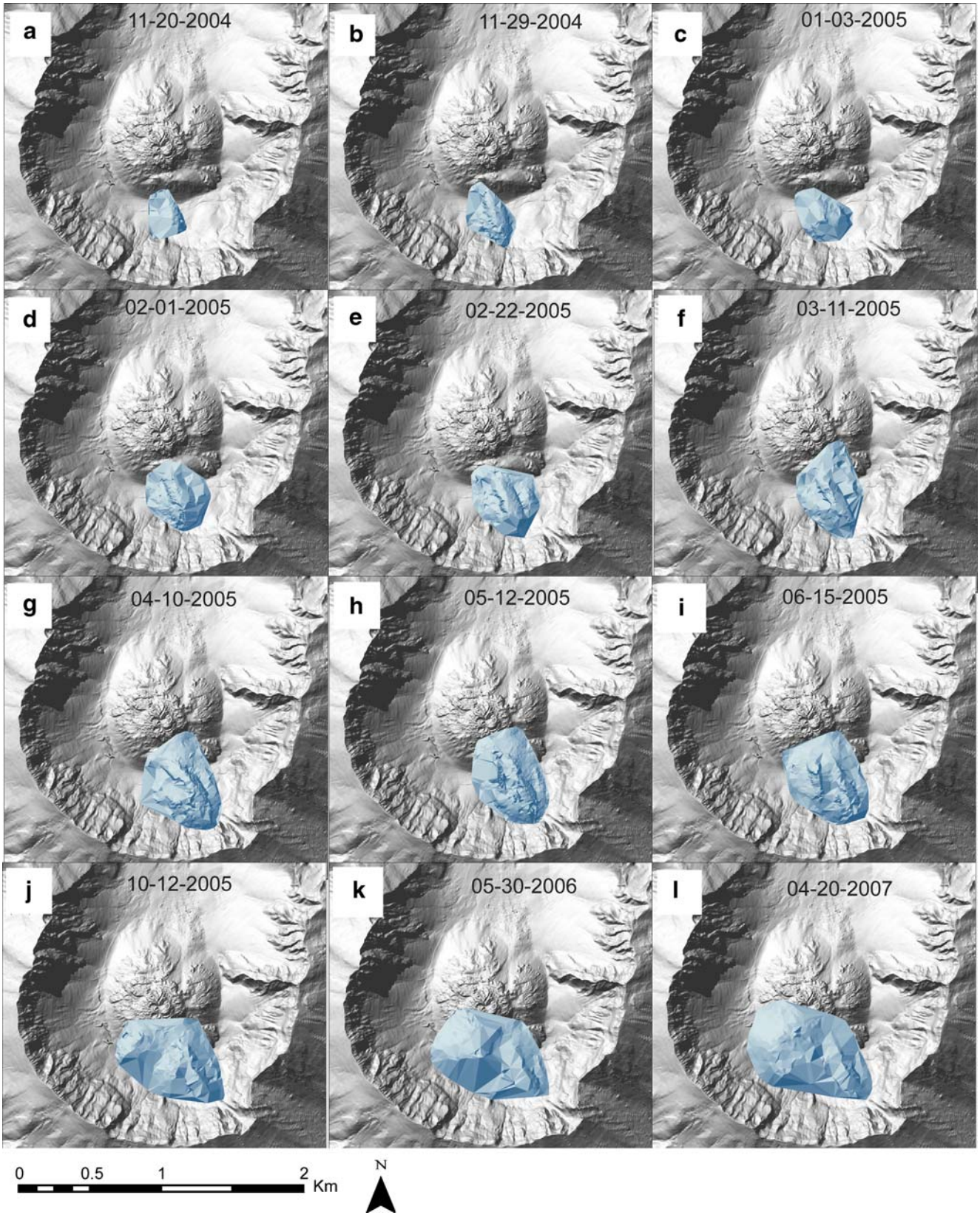

Fig. 3 Sequence of shaded relief depictions of DEMs (**a–l**) produced by oblique photogrammetry (*blue scale*) overlain on DEM from 1986 (*gray scale*) derived from vertical photogrammetry. Dates span November 2004 to April 2007

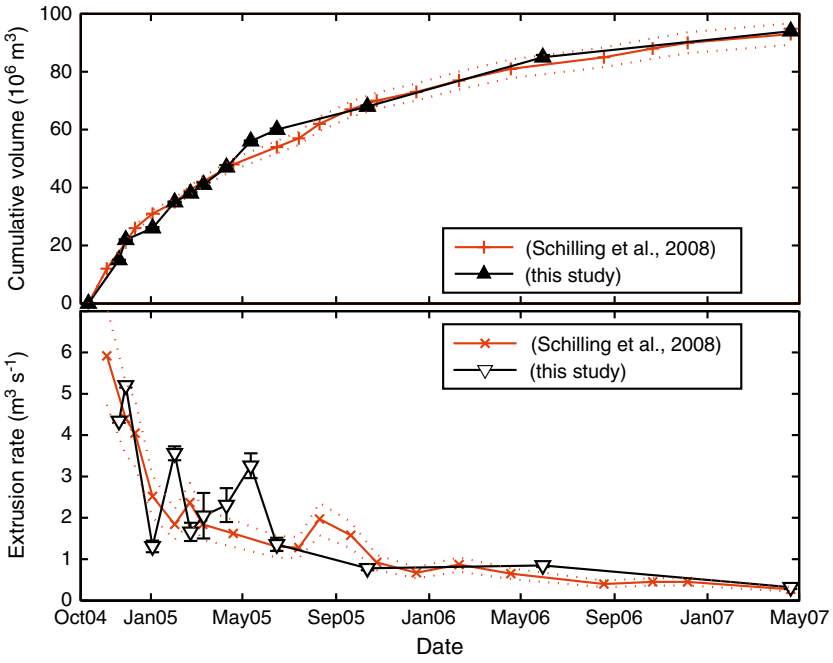

Fig. 4 Time series of dome volume (*upper*) and extrusion rates (*lower*) calculated from DEMs derived from oblique photogrammetry compared to those derived from vertical photogrammetry (cf Table 1). *Dotted lines* show 4% uncertainty in volumes reported by Schilling et al. (2008), and 20% variation in their reported flux rates. Reported uncertainties of flux rates estimated by Schilling et al. (2008) are approximately the size of the symbols

From October 2005 to April 2007, extrusion rates remained relatively constant at <1 m^3/s (Fig. 4). Between June and October, 2005, spine 6 emerged more than 200 m west–northwest of the previous spine and endogenous growth (growth from within the talus, i.e., inflation) dominated the character of eruptive activity (Fig. 3i–j). Seven months elapsed before another oblique photogrammetry flight on May 30, 2006, which captured spine 7 (Fig. 3k). The new dome had essentially filled the entire area of the crater floor south of the 1980–1986 dome; the volume of the new dome had reached 85×10^6 m^3 (Figs. 3k and 4). Nearly a year later, on April 20, 2007, the final set of oblique aerial photographs shows endogenous growth continued to dominate. The west section of the new dome decreased over 60 m in elevation but continued to grow in circumference to an average diameter of 500 m (Fig. 3l). Two and a half years of dome growth formed a composite lava dome with a total volume of 94×10^6 m^3 (Figs. 3l and 4), which is slightly larger than the 1980–1986 dome (Swanson and Holcomb 1990). By this time, the extrusion rate had declined to 0.3 m^3/s; its lowest level since the onset of eruption in October 2004 (Fig. 4).

Discussion

Accuracy assessment

We can assess the accuracy of this rapid, low-cost oblique photogrammetry technique by comparing estimates of volume and extrusion rate to those from conventional vertical photogrammetry made during the same interval. Figure 4 shows a direct comparison of lava dome volume and extrusion rate calculated by both techniques. Each DEM yields reasonable estimates of dome growth as compared to the results obtained by traditional photogrammetry (volume and extrusion rate; Table 1).

Total dome volume estimates measured by the two techniques fall within each method's uncertainty, with three exceptions. The discrepancies on November 20, 2004, January 3, 2005, and June 15, 2005, can be attributed to adverse atmospheric effects resulting in insufficient photographic coverage for one or both methods. On average, volume calculations from the oblique photogrammetry DEMs were within 5% of volume calculations from vertical photogrammetry DEMs. The small discrepancies in volume estimates between the two techniques can lead to larger differences in our estimates of extrusion rate. The wavelength variation in the average extrusion rate shown in Fig. 4 is probably not meaningful, but the overall nonlinear trend of decreasing extrusion rate through time is captured by both photogrammetric techniques.

Oblique photogrammetry can yield volume and extrusion rate estimates quickly and relatively safely for rapid hazard evaluation at an active volcano. A new DEM can be constructed from a set of oblique photos in a few hours. The most labor-intensive aspect of the process is manual identification of reference points from pairs or series of photographs. As the dome grew larger each successive photogrammetry model required more three-dimensional points to accurately represent its morphology. For an extremely rapid assessment of volumes and extrusion rates, relatively few points are required: a good perimeter (points that outline the area of interest) and as few as one (highest

elevation) point in the interior of the dome. This approach depends on the complexity of the terrain being modeled, the scale, and the accuracy objectives of the given project. A better representation of the form of the dome and more accurate volume measurements require a more dense point cloud (i.e., as many points as can be located given the resolution of the image).

Conclusion

This study successfully applied oblique photogrammetry to measure dome growth at MSH. The technique used oblique aerial photographs to create successive DEMs for qualitative and quantitative descriptions of dome growth during the 2004–2008 eruption. The DEMs were used to calculate dome volume and extrusion rate, and to track changes in these quantities through time. We show that extrusion rates, initially on the order of 5 m^3/s, decreased through time to less than 1 m^3/s from November 2004 through April 2007, and that by April 2007 dome volume had reached 94×10^6 m^3. These results are within 5% of those obtained through traditional photogrammetry by Schilling et al. (2008).

Considering the ever-increasing improvements in camera technology, commercially available software solutions, and computer processing speeds, this method of oblique photogrammetry shows promise as a cost- and time-efficient tool for volcano monitoring. It can yield rapid and simple surveys that produce results sufficiently accurate for efficient monitoring and quantification of large-scale deformation and lava effusion during volcanic eruptions. Oblique photogrammetry also shows promise for surveying areas that are not easily accessible, and for enabling rapid data processing in the field or at a temporary office location with only a laptop computer, desirable when timely hazard-mitigation information is needed.

Acknowledgments The authors wish to thank the USGS Volcano Hazards Program, the Cascades Volcano Observatory and Western Washington University for jointly supporting this study. We thank S. Linneman and J.Caplan-Auerbach for comments on an earlier version of this manuscript and R. Herd for insightful discussions. The manuscript was improved by reviews from P. Baldi, A. Stinton, J. Pallister, and J. Major. Diefenbach was supported in this work by a Jack Kleinman Grant from the USGS Cascades Volcano Observatory, a National Science Foundation Graduate K-12 Fellowship through WWU, a Mazamas Graduate Student Research Grant, and WWU Geology Department and Graduate Studies grants.

References

Achilli V, Baldi P, Baratin L, Bonin C, Ercolani E, Gandolfi S, Anzidei M, Riguzzi F (1998) Digital photogrammetric survey on the island of Vulcano. Acta Vulcanol 10:1–5

Baldi P, Bonvalot S, Briole P, Marsella M (2000) Digital photogrammetry and kinematic GPS applied to the monitoring of Vulcano Island, Aeolian Arc, Italy. Geophys J Int 142:801–811

Baldi P, Bonvalot S, Briole P, Coltelli M, Gwinner K, Marsella M, Puglisi G, Remy D (2002) Validation and comparison of different techniques for the derivation of digital elevation models and volcanic monitoring (Vulcano Island, Italy). Int J Rem Sens 23:4739–4800

Bluth GJS, Rose WI (2004) Observations of eruptive activity at Santiaguito volcano, Guatemala. J Volcanol Geotherm Res 136:297–302

Calder ES, Luckett R, Sparks RSJ, Voight B (2002) Mechanisms of lava dome instability and generation of rockfalls and pyroclastic flows at Soufrière Hills Volcano, Montserrat. In: Druitt TH, Kokelaar BP (eds) The eruption of Soufrire Hills volcano, Montserrat, from 1995 to 1999. Geol Soc Lond Mem, 21:173–190

Cecchi E, van Wyk de Vries B, Lavest JM, Harris A, Davies M (2003) N-view reconstruction: a new method for morphological modeling and deformation measurement in volcanology. J Volcanol Geotherm Res 123:181–201

Diefenbach AK (2007) Oblique photogrammetric analysis of the dome-building eruption of Mount St. Helens, 2004–2007: MS thesis, Western Washington University, 103 p

Harris AJL, Murray JB, Aries SE, Davies MA, Flynn LP, Wooster MJ, Wright R, Rothery DA (2000) Effusion rate trends at Etna and Krafla and their implications for eruptive mechanisms. J Volcanol Geotherm Res 102:237–269

Harris AJL, Rose WI, Flynn LP (2003) Temporal trends in lava dome extrusion at Santiaguito 1922–2000. Bull Volcanol 65:77–89

Herd RA, Edmonds M, Bass VA (2005) Catastrophic lava dome failure at Soufriere Hills Volcano, Montserrat, 12–13 July 2003. J Volcanol Geotherm Res 148:234–252

Honda K, Nagai M (2002) Real-time volcano activity mapping using ground-based digital imagery. ISPRS J Photogramm Remote Sens 57:159–168

Iverson RM (2008) Dynamics of seismogenic volcanic extrusion resisted by a solid surface plug, Mount St. Helens, 2004–2005. In: Sherrod DR, Scott WE, Stauffer PH (eds) A Volcano Rekindled: The Renewed Eruption of Mount St. Helens, 2004–2006. US Geol Surv Prof Pap 1750:425–460

Iverson RM, Dzurisin D, Gardner CA, Gerlach TM, LaHusen RG, Lisowski M, Major JJ, Malone SD, Messerich JA, Moran SC, Pallister JS, Qamar AI, Schilling SP, Vallance JW (2006) Dynamics of seismogenic volcanic extrusion at Mount St. Helens in 2004–05. Nature 444:439–443

James MR, Robson S, Pinkerton H, Ball M (2006) Oblique photogrammetry with visible and thermal images of active lava flows. Bull Volcanol 69:105–108

James MR, Pinkerton H, Robson S (2007) Image-based measurements of flux variation in distal regions of active lava flows. Geochem Geophys Geosyst 8:Q03006

Jordan R, Kieffer HH (1981) Topographic changes at Mount St. Helens : large-scale photogrammetry and digital terrain models. In: Lipman PW, Mullineaux DR (eds) The 1980 eruptions of Mount St. Helens, Washington. US Geol Surv Prof Pap 1250:135–141

Julio-Miranda P, Delgado-Granados H (2003) Fast hazards evaluation employing digital photogrammetry: Popocatépetl glaciers, México. Geof Int 42:275–283

Kaneko T, Wooster M, Nakada S (2002) Exogenous and endogenous growth of the Unzen lava dome examined by satellite infrared image analysis. J Volcanol Geotherm Res 116:151–160

Kerle N (2002) Volume estimation of the 1998 flank collapse at Casita volcano, Nicaragua—a comparison of photogrammetric and conventional techniques. Earth Surf Process Landforms 27:759–771

Major JJ, Kingsbury CG, Poland MP, LaHusen RG (2008) Extrusion rate of the Mount St. Helens lava dome estimated from terrestrial imagery: November 2004-December 2005. In: Sherrod DR, Scott WE, Stauffer PH (eds) A Volcano Rekindled: The Renewed Eruption of Mount St. Helens, 2004–2006. US Geol Surv Prof Pap 1750:237–255

Major JJ, Dzurisin D, Schilling SP, Poland MP (2009) Monitoring lava-dome growth during the 2004–2008 Mount St. Helens, Washington, eruption using oblique terrestrial photography. Earth Plan Sci Lett 286:243–254

Mills HH (1992) Post-eruption erosion and deposition in the 1980 crater of Mount St. Helens, Washington, determined from digital maps. Earth Surf Process Landforms 17:739–754

Moore JG, Albee WC (1981) Topographic and structural changes, March–July 1980—photogrammetric data. In: Lipman PW, Mullineaux DR (eds) The 1980 eruptions of Mount St. Helens, Washington. US Geol Surv Prof Pap 1250:123–134

Poland MP, Dzurisin D, LaHusen RG, Major JJ, Lapcewich D, Endo ET, Gooding DJ, Schilling SP, Janda CG (2008) Remote camera observations of lava dome growth at Mount St. Helens, Washington, October 2004 to February 2006. In: Sherrod DR, Scott WE, Stauffer PH (eds) A Volcano Rekindled: The Renewed Eruption of Mount St. Helens, 2004–2006. US Geol Surv Prof Pap 1750:225–236

Pyle DM, Elliott JR (2006) Quantitative morphology, recent evolution, and future activity of the Kameni Islands volcano, Santorini, Greece. Geosphere 2:253–268

Ryan GA, Loughlin SC, James MR, Jones LD, Calder ES, Christopher T, Strutt MH, Wadge G (2010) Growth of the lava dome and extrusion rates at Soufrière Hills Volcano, Montserrat, West Indies: 2005–2008. Geophys Res Lett 37:L00E08. doi:10.1029/2009GL041477

Schilling SP, Carrara PE, Thompson RA, Iwatsubo EY (2004) Posteruption glacier development within the crater of Mount St. Helens, Washington, USA. Quat Res 61:325–329

Schilling SP, Thompson RA, Messerich JA, Iwatsubo EY (2008) Use of digital aerophotogrammetry to determine rates of lava dome growth, Mount St. Helens, 2004–2005. In: Sherrod DR, Scott WE, Stauffer PH (eds) A Volcano Rekindled: The Renewed Eruption of Mount St. Helens, 2004–2006. US Geol Surv Prof Pap 1750:145–167

Scott WE, Sherrod DR, Gardner CA (2008) Overview of the 2004 to 2005, and continuing, eruption of Mount St. Helens, Washington. In: Sherrod DR, Scott WE, Stauffer PH (eds) A Volcano Rekindled: The Renewed Eruption of Mount St. Helens, 2004–2006. US Geol Surv Prof Pap 1750:3–22

Stevens NF (2002) Emplacement of the large andesite lava flow in the Oturere Stream valley, Tongariro Volcano, from airborne interferometric radar, New Zealand. J Geol Geophys 45:387–394

Stoer J, Bulirsch R (2002) Introduction to numerical analysis. Springer, Berlin, pp 9–36

Swanson DA, Holcomb RT (1990) Regularities in growth of the Mount St. Helens Dacite Dome, 1980–1986. In: Fink J (ed) The Mechanics of Lava Flow Emplacement and Dome Growth. IAVCEI Proc Volcanol 2:1–18

Thompson RA, Schilling SP (2007) Photogrammetry. In: Dzurisin D (ed) Volcano deformation—geodetic monitoring techniques. Springer-Praxis Books in Geophysical Sciences, Berlin, pp 195–221

Vallance JW, Schneider DJ, Schilling SP (2008) Growth of the 2004–2006 lava-dome complex at Mount St. Helens, Washington. In: Sherrod DR, Scott WE, Stauffer PH (eds) A Volcano Rekindled: The Renewed Eruption of Mount St. Helens, 2004–2006. US Geol Surv Prof Pap 1750:169–208

Wadge G (2003) Measuring the Rate of Lava Effusion by InSAR. Proc FRINGE Workshop ESA SP-550:34.1

Wadge G, Dorta D, Cole P (2006) The magma budget of Volcán Arenal, Costa Rica from 1980 to 2004. J Volcanol Geotherm Res 157:60–74

Zlotnicki J, Ruegg JC, Bachelery P, Blum PA (1990) Eruptive mechanism on Piton de la Fournaise volcano associated with the December 4, 1983, and January 18, 1984 eruptions from ground deformation monitoring and photogrammetric surveys. J Volcanol Geotherm Res 40:197–217